Branched Polymers and their Application in Corrosion Inhibition for Mild Steel in 1M H$_2$SO$_4$ Medium

P. SOUNTHARI, A. KIRUTHIKA, J. SARANYA, K. PARAMESWARI and S. CHITRA*

Department of Chemistry, P.S.G.R.Krishnammal College for Women,
Peelamedu, Coimbatore - 641004, India.
*Corresponding author E-mail: rajshree1995@rediffmail.com

ABSTRACT

The adsorption and corrosion inhibiting effect of branched polymers (BATP, BAAZ, BETP & BEAZ) on mild steel in 1M H$_2$SO$_4$ at 30±1°C was investigated using gravimetric, electrochemical impedance spectroscopy (EIS), and potentiodynamic polarization techniques. The experimental findings revealed that BATP inhibited the corrosion reaction in the acid environment to greater extend compared to BAAZ, BETP and BEAZ. Impedance results indicate that the polymers were adsorbed on the metal/solution interface, while polarization data showed that the polymers behaved mostly as mixed-type inhibitors. Kinetic parameters (activation energy, pre-exponential factor, enthalpy of activation and entropy of activation) as well as thermodynamic parameters (enthalpy of adsorption, entropy of adsorption and Gibbs free energy) were calculated and discussed. Scanning electron microscopy technique was used to confirm the effectiveness of inhibition of mild steel in sulphuric acid medium.

Key words: Branched polymers, thermal studies, electrochemical techniques, SEM, AAS,

INTRODUCTION

Iron and its alloys find utility in a wide spread spectrum of many industrial units because of its low-cost and excellent mechanical properties. For this reason, the corrosion behavior of these materials has attracted the attention of several investigations. Steel is the most corrosion vulnerable metal. Thus, much attention is given for its protection from the hostile environments. Acid solutions are widely used in industry. The most important areas of application are acid pickling, industrial acid cleaning, acid descaling, and oil-well acidizing[1-3]. Organic compounds containing polar functional groups such as nitrogen, sulphur, and/or oxygen in a conjugated system have been reported to be effective corrosion inhibitors for steel[4-6]. Some of the organic compounds are polymeric in nature and therefore possess multiple active centres. The study of corrosion inhibition by polymers has been on the increase in recent times. Polymers are employed as corrosion inhibitors because the

presences of many adsorption centres help them form complexes with metal ions. The formed complexes are adsorbed on the metal surface to form a barrier film which separated the metal surface from the corrosive agents present in the aggressive solution. The improved performances of polymeric materials are attributed to their multiple adsorption sites for bonding with metal surface. The main advantages of polymeric inhibitors are (i) a single polymeric chain displaces many water molecules from the metal surface thus making the process entropically favorable (ii) the presence of multiple bonding sites makes the desorption of polymers a slower process. Furthermore it has been noticed that both the molecular area and molecular weight of the inhibitor are of key importance[7-12]. Some authors have reported on the effectiveness of polymeric corrosion inhibitors[13-17]. According to them, the inhibitive power of the polymers is related structurally to the cyclic rings and heteroatoms which are the major active centres of adsorption.

From the review of literature, it is evident, that practically no work has so far been reported with regard to the inhibition of acid corrosion of mild steel by branched polymers.

This paper is focused on the synthesis, characterization, and potential use of a new class of branched polymers used as corrosion inhibitors for mild steel in 1M H_2SO_4 medium.

EXPERIMENTAL

Synthesis of branched polymers and polyamides Monomers
Synthesis of oxadiazole monomer[18]

Polyphosphoric acid (0.5mole) was taken in a round bottom flask .To this (0.1mole) of hydrazine hydrate was added in drops, for 15 minutes with stirring, while maintaining the flask on ice water bath. To this mixture 0.1mole of 3,5-diamino benzoic acid was added and refluxed for 6-7 hours at 130°C and then cooled at 70°C. The mixture was poured with stirring into ice. The precipitate obtained was filtered and washed with sodium carbonate in order to remove excess polyphosphoric acid. The 2,5-bis(3,5-diaminophenyl)-1,3,4-oxadiazole (TAPO) was recrystallized from ethanol. The product was characterized by IR spectra.
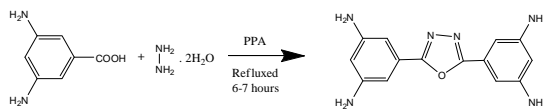
Synthesis of aromatic diacid chloride:[19]

15g of terephthalic acid was refluxed for about 4 hours with 70 ml of thionyl chloride in the presence of 2 drops of pyridine as a catalyst until a clear solution was obtained. The colourless solid thus obtained was recrystallized from dry benzene. The solid obtained was used as such for polymerization process.

Synthesis of aliphatic diacid chloride:[19]

Crystallized azeloic acid 14.6g and 27ml distilled thionyl chloride was refluxed in an oil bath for 4 hours. After refluxing, the solid acid chloride obtained on cooling was filtered, dried and the acid chloride was used as such.

Synthesis of branched polyamides [20]

The poly condensation reaction of 2,5-bis(3,5-diaminophenyl)-1,3,4-oxadiazole (0.1M) with diacid chloride (0.4M) was carried out in N-methyl pyrrolidinone (NMP) using pyridine as an acid acceptor.

Poly condensation was run by adding powdered diacid chloride (0.1M) to a solution of the (TAPO) tetraamine with stirring, under nitrogen, at -5°C. After addition of the diacid chloride, the reaction mixture was kept at -5°C for 30 minutes, then the temperature was allowed to increase to room temperature by removing the cooling bath, and the solution was further stirred for 4 hours. The polymer
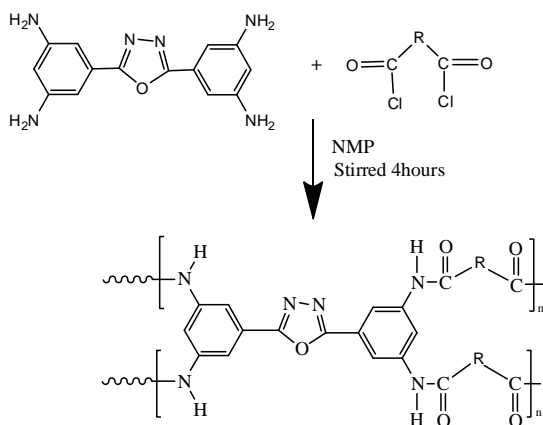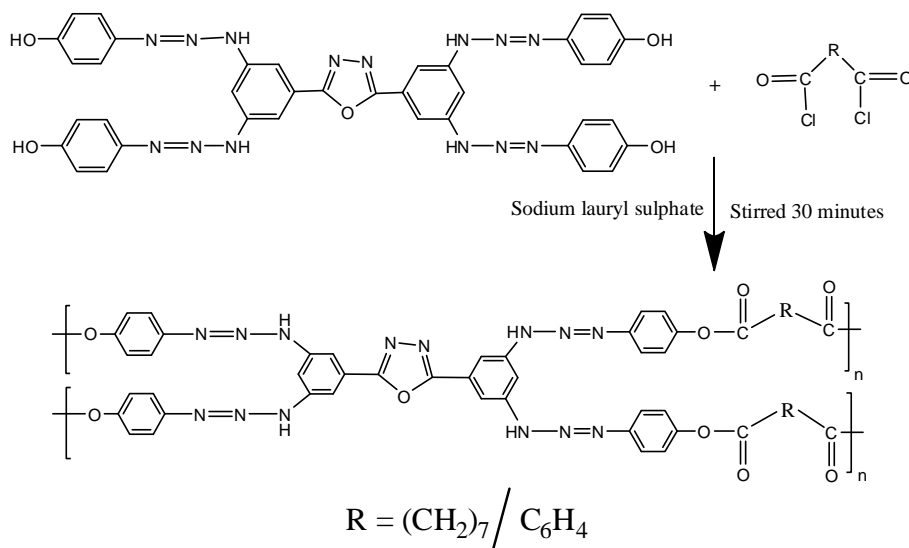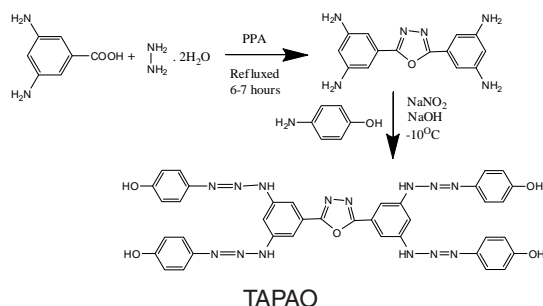

Scheme 1:

solution was diluted to about 5% by addition of more NMP and the polymer was precipitated by pouring into water. It was filtered, washed twice with water and once with ethanol, and dried. The reaction sequence is shown in scheme 1.

Synthesis of branched polyesters
Synthesis of monomers

The oxadiazole monomer was synthesized by the reaction of 3,5-diamino benzoic acid with hydrazine hydrate in polyphosphoric acid (PPA)[18]. In the second step, 0.01M of 2,5-bis(3,5-diaminophenyl)-1,3,4-oxadiazole was dissolved in

NaOH (10%) and to this solution, the diazonium salt solution(4-amino phenol and $NaNO_2$) was added over a period of 25minutes and the mixture was stirred for three hours. The resulting red-orange suspension was acidified with dilute HCl and the product obtained was filtered, followed by washing with hot water and dilute HCl. Then the product (monomer I) was taken as monomer for polymerization[19].

Synthesis of aliphatic diacid chloride:[19]

The above mentioned procedure was followed for the synthesis of aromatic/aliphatic acid chlorides.

Synthesis of branched polyesters

Small amount of monomer I was dissolved in 10% NaOH solution. To this small amount of sodium lauryl sulphate was added and stirred for half an hour. Then approximately 5ml of acid chloride was added followed by the addition of chloroform and acetone[19]. The reaction sequence is shown in scheme 2.

TAPAO

$$R = (CH_2)_7 \Big/ C_6H_4$$

Scheme 2:

The structures of the synthesized polymers were confirmed by IR spectra using Shimadzu IR Affinity 1 [Figs.1&2]. NMR spectrum of branched polymers was recorded in DMSO-d_6 using a 400 MHz NMR spectrometer (Bruker, DPX-400) [Figs. 3&4]. In order to determine the thermal stability of

the polymers, thermograms of the polymers was recorded in dynamic nitrogen atmosphere with a heating rate of 10°C using a Perkin Elmer (TGS-2 model) thermal analyzer [Figs. 5&6].In order to determine the glass transition temperature DSC of the polymers was recorded using PerkinElmer

precisely, Diamond differential scanning calorimeter [Figs. 7&8]. The percentage crystallinity of the synthesized polymers was determined by wide angle XRD using Brucker XRD at STIC, CUSAT, Cochin [Fig.9].

Evaluation of Inhibition Efficiency of the branched polymers
Non-Electrochemical Techniques
Weight loss method

Gravimetric corrosion measurements were carried out according to the ASTM standard procedure. The initial weight of the polished mild steel plates were taken.1M H_2SO_4 was taken in an 100 ml beakers and the specimens were suspended in triplicates into the solution using glass hooks. Care was taken to ensure the complete immersion of the plates. After a period of 3 hours the plates were removed, washed with distilled water, dried and weighed. From the initial and final masses of the plates (i.e., before and after immersion in the solution) the loss in weight was calculated. The experiment was repeated for various inhibitor concentrations in 1M H_2SO_4. To study the effect of temperature, the above procedure was carried out at different temperature range i.e., (303-333K) using thermostat with the inhibitor concentration of 1000ppm.

Atomic Absorption Spectroscopy (AAS)

Atomic Absorption Spectrophotometer (Model GBC 908, Australia) was used for estimating the amount of dissolved iron in the corrodent solution containing various concentrations of polymers in 1M H_2SO_4 after exposing the mild steel specimen for 3 hours. From the amount of dissolved iron, the inhibitor efficiency was calculated.

Surface Morphology

Surface examinations of mild steel specimens were carried out to understand the surface morphology of mild steel in 1M H_2SO_4 in the presence and absence of the inhibitors using Medzer biomedical research microscope (Mumbai, India).

Electro chemical Techniques
Impedance spectroscopy

The electrochemical measurements were performed in a classical three-electrode cell assembly with mild steel rod (exposed area 0.78 cm^2) as working electrode, a platinum electrode and saturated calomel electrode as counter and reference electrodes. The measurements were carried out with IVIUM Compactstat Potentiostat/ Galvanostat. EIS measurements were carried out at a frequency range of 10 KHz to 0.01Hz with a superimposed sine wave of amplitude 10mV. From the plot of Z^1 Vs Z^{11} the charge transfer resistance (R_{ct}) and double layer capacitance (C_{dl}) were calculated.

Potentiodynamic polarization

Polarization studies were carried out for the mild steel specimens in 1M H_2SO_4 in the absence and presence of the inhibitors to evaluate the corrosion kinetic parameters I_{corr}, E_{corr} and Tafel slopes b_a and b_c. The electrochemical unit and cell used for impedance measurements were also used for polarization measurements. The measurements were carried out from a potential range -200mV to +200mV with respect to the open circuit potential, at a scan rate of 1mV/sec.

RESULTS AND DISCUSSION

Characterization of branched polymers

The synthesized polymers are presented in Table 1.

Infra-red spectra

The structures of the polymers were confirmed by FT-IR spectra. The FT-IR spectrum of the monomer TAPO shows (Fig. 1a), the presence of bands at 3360 cm^{-1}(-NH_2), 1605 cm^{-1} (-C=N-) and 1019 cm^{-1}(-C-O-C-) respectively confirming the presence of these groups in 1,3,4-oxadiazole ring [21]. Whereas in the IR spectrum of the polyamides (Fig.1b) by disappearance of absorption band at 3360cm^{-1}(-NH_2) and appearance of sharp band at 1687-1704 cm^{-1} for carbonyl group confirmed the formation of the polyamides. Presence of absorption bands at 1473-1578 cm^{-1} (-C=N-), 3063-2931 cm^{-1} (-NH stretching) and 1019-1012 cm^{-1} (-C-O-C-) further confirmed the structure of the polyamides BATP and BAAZ.

In the IR spectrum of monomer TAPAO a broad band was observed at 3254 cm^{-1} which is due to the presence –OH group (Fig.2a). In the

polyester (Fig.2b) the broad peak due to –OH disappeared and sharp peak around 1690 cm^{-1} confirmed the presence of –COO- group. The presence of (-C=N-) and (-N=N-) was observed at frequency 1512-1468 and 1413cm^{-1} respectively. (-C-O-C-) stretching of 1,3,4-oxadiazole ring appeared at 1020-1090cm^{-1} which confirmed the structure of the polyesters(BETP and BEAZ).
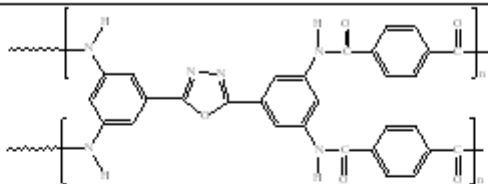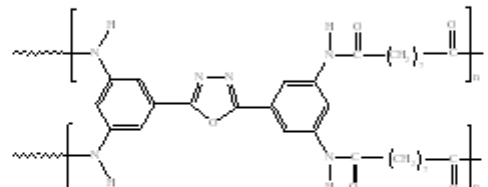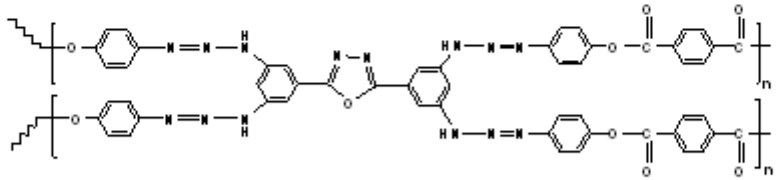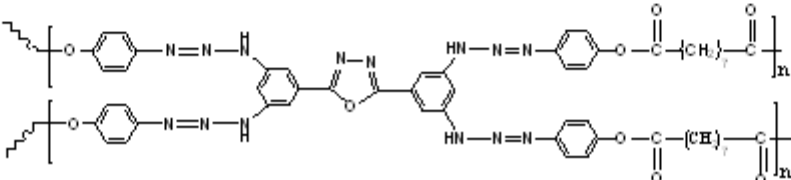
^{1}HNMR studies

^{1}H-NMR δ_H (d$_6$ - DMSO), 400 MHz of the polyester BETP (Fig.3) showed peaks at about 9.932 (s, 2H, NH), 8.267-8.246(d, 4H, phenyl), 8.159-8.138 (d, 4H, phenyl), 7.217 – 7.286 (d, 4H, phenyl), 6.872 – 6.936(d, 4H, phenyl), 5.684(s, -CH$_2$-). Branched polyamide BATP (Fig.4) showed peaks at about 9.77 (s, 2H, NH), 8.132-8.146(d, 4H, phenyl), 7.77-7.75 (d, 4H, phenyl), 6.96-6.94 (d, 4H, phenyl) 8.09 (s, -CH$_2$-).

Thermal analysis

Thermal stability of the polymers was studied by therrmogravimetric analysis. Their decomposition, in nitrogen, begins at about 250 ÚC except BATP as indicated by the temperature of 10% weight loss in TGA thermograms (Table 3). Typical therrmogravimetric curves of these polymers are shown in Fig.5 and 6. Thermal stability of polymers was in the order of BETP> BATP>BEAZ>BAAZ. The results obtained from thermal studies showed that the fully aromatic one is more stable than the semi aromatic polymers. The char yields of polymers at 700°C were about 1.1-47.2%. The results are given in Table 3. The

Table 1: Structure of the branched polymers

S.NO	Structure of the branched polymers	Yield (%)
1.	BATP	90
2.	BAAZ	89
3.	BETP	87
4.	BEAZ	84

results reveal that, synthesized polyesters have high thermal stability than polyamides. The fully aromatic polymers showed better stability than semi-aromatic ones. The higher thermal stability of polymer BETP could be attributed to the incorporation of azomethine, oxadiazole ring and fully aromatic nature of the polymer backbone. The higher thermal stability is due to the intense chain stiffness and intermolecular hydrogen bonding of azomethine groups between the neighboring chains. Introduction of performed oxadiazole ring, phenylation of polymer backbone and symmetry of the structures are the most important structural modifications for increase in thermal stability (char % yield 47.2 at 800°)[22]. The glass transition temperature of the polymers is in the range of 88-151°C (Table 3).

X-ray studies:

Wide-angle X-ray diffraction of the polymers is shown in Fig.9. On the basis of X-ray diffraction studies, it has been found that all the newly synthesized polymers of 1,3,4-oxadiazole are crystalline nature except the polyamide BAAZ which is amorphous.

Inhibition efficiency of the polymers
Weight loss method

The weight loss experiment is a base line method to observe optimum concentration after

Table 2: IR stretching frequencies of some synthesized monomers and branched polymers

Name of the sample	Stretching frequencies in cm^{-1}		
	υ_{-NH2}	**3360**	
Monomer	-C=N-	1605	
(TAPO)	-C-O-C-	1019	
		BATP	BAAZ
	-NH	3063	2931
Polyamides	-C=N-	1578	1473
	-C=O-	1687	1704
	-C-O-C-	1019	1012
Monomer	-OH	3254	
	-C=N-	1600	
(TAPAO)	-C-O-C-	1015	
	-N=N-	1512	
		BETP	BEAZ
	-C=N-	1512	1468
Polyesters	-C-O-C-	1020	1090
	-N=N-	1413	1413
	-C-O-C ‖ O	1687	1687

Table 3: Thermal properties of the polymers:

Name of Polymers	T_g (°C)	T_{10} (°C)	T_{20} (°C)	T_{max}(°C)	Char yield (%)
BATP	148	139	170	380	3.2
BAAZ	150	249	320	355	9.9
BETP	151	319	364	634	47.2
BEAZ	88	269	284	358	1.1

which there is no remarkable change in the inhibition efficiency. This may be due to the adsorption of   polymers leading to the formation of a smooth layer on metal surface which prevents the contact of metal with the surrounding acidic environment and higher bonding ability of inhibitor on the mild steel surface. Data obtained for mild steel in 1M H_2SO_4 at 30±1°C in presence and absence of different concentrations of inhibitors is summarized in Table 4 (Fig. 10).The corrosion rate values of mild steel in 1M H_2SO_4 decreases as the concentration of polymers increases[23-24]. Adsorption process of an inhibitor depends upon its nature such as planarity of compound, lone pairs present in hetero atoms, multiple bonds etc. The addition of polymers results in rapid formation of a protective layer on metal surface through metal/solution interface[25,26]. From Table 4, it is also evident that the order of increase in inhibition efficiency is BATP> BAAZ>BETP>BEAZ. This implies that aromatic branched polyamide has the highest inhibition

efficiency while aliphatic branched polyester has the least.

Temperature studies

The effect of temperature on the inhibited acid–metal reaction is very complex, because many changes occur on the metal surface such as rapid etching and desorption of inhibitor and the inhibitor itself may undergo decomposition[27]. The change of the corrosion rate with the temperature was studied in 1M H_2SO_4, both in absence and presence of branched polyamides and polyesters and is presented in Table 5. The effect of temperature on the corrosion parameter of mild steel in 1M H_2SO_4 was studied at 303, 313, 323 and 333K. The results indicate that as the temperature increases the corrosion rate increases and inhibition efficiency decreases. The mechanism of inhibition can be deduced by comparing the activation energy in the presence and absence of the inhibitor. The Arrhenius plot and transition state plot were used

Table 4: Inhibition efficiencies of various concentrations of the inhibitors for corrosion of mild steel in 1M H_2SO_4 obtained by weight loss measurement at 30±1⁰C

Name of the inhibitors	Concentration (ppm)	Weight loss (g)	Inhibition Efficiency (%)	Degree of surface coverage(θ)	Corrosion rate $(gcm^{-2}h^{-1})$
Blank	-	0.2209	-	-	14.31
BATP	10	0.1235	44.1	0.4409	8.00
	50	0.0722	67.3	0.6732	4.68
	100	0.0482	78.2	0.7818	3.12
	500	0.0252	88.6	0.8859	1.63
	1000	0.0116	94.7	0.9475	0.75
BAAZ	10	0.1595	27.8	0.2780	10.33
	50	0.0964	56.4	0.5636	6.25
	100	0.0721	67.4	0.6736	4.67
	500	0.0487	80.0	0.7795	3.16
	1000	0.0362	83.6	0.8361	2.35
BETP	10	0.1638	25.8	0.2585	10.61
	50	0.1045	52.7	0.5269	6.77
	100	0.0836	62.2	0.6215	5.42
	500	0.0558	74.7	0.7474	3.62
	1000	0.0446	79.8	0.7981	2.89
BEAZ	10	0.1786	19.1	0.1915	11.57
	50	0.1136	48.6	0.4857	7.35
	100	0.0887	59.8	0.5985	5.74
	500	0.0656	70.3	0.7030	4.25
	1000	0.0538	75.6	0.7565	3.48

to determine the activation energy (Ea), activation enthalpy ($\Delta H°$), and activation entropy ($\Delta S°$) for the corrosion of mild steel in 1M H_2SO_4 with and without polymers. The activation energy can be obtained by the Arrhenius equation and Arrhenius plot:

$$...(1)$$

where E_a is the activation energy, R is the universal gas constant, K is the pre-exponential constant and T is the absolute temperature.

In an attempt to elucidate the enthalpy of activation ΔH^0, and entropy of activation ΔS^0 the following transition state equation was used:

Corrosion rate $\hspace{3cm}$ ...(**2**)

where h is the Planck constant, N is the Avogadro number, R is the universal gas constant, ΔH^0 is the enthalpy of activation, and ΔS^0 is the entropy of activation respectively. For this purpose, relationship of log corrosion rate and 1/T is

Table: 5 Inhibition efficiencies of 1000 ppm concentrations of the inhibitors for corrosion of mild steel in 1M H_2SO_4 obtained by weight loss measurement at higher temperature

Name of the inhibitor	Temperature (K)	Weight loss(g)	Inhibition efficiency (%)	Corrosion rate (mpy)
Blank	303	0.0736	-	1.75
	313	0.1350	-	0.13
	323	0.1979	-	0.19
	333	0.2846	-	0.28
BATP	303	0.0239	67.5	0.56
	313	0.0564	58.2	1.34
	323	0.1114	43.7	2.65
	333	0.1988	30.1	4.73
BAAZ	303	0.0262	64.4	0.62
	313	0.0596	55.8	1.41
	323	0.1154	41.6	2.74
	333	0.1976	30.6	4.70
BETP	303	0.0286	61.1	0.68
	313	0.0648	52.0	1.54
	323	0.1244	37.1	2.96
	333	0.2178	23.5	5.18
BEAZ	303	0.0306	58.4	0.72
	313	0.0662	50.9	1.57
	323	0.1292	34.7	3.08
	333	0.2266	20.3	5.39

Table: 6 Kinetics/Thermodynamic Parameters of mild steel corrosion in 1M H_2SO_4

Name of the inhibitor	E_a (kJ)	$-\Delta G^0_{ads}$(kJ)				$-\Delta H^0$ kJ/mole	$-\Delta S^0$ kJ/mole
		303 K	313 K	323K	333 K		
Blank	37.36	-	-	-	-	-	-
BATP	59.15	31.12	31.10	30.52	29.84	84.09	0.75
BAAZ	56.52	33.81	32.82	31.24	29.90	256.75	1.27
BETP	56.68	33.42	32.39	30.71	28.90	293.72	1.39
BEAZ	56.08	33.11	32.28	30.42	28.40	307.51	1.44

illustrated in Fig.11. The slope and intercept of the straight line are ($\Delta H^0/2.303R$) and (log(R/Nh) + ($\Delta S^0/2.303R$)), respectively. These are used to compute the values of ΔH^0 and ΔS^0, respectively, and the data are compiled in Table 6.

From Table 6, it is clear that the activation energy E_a increases in the presence of the inhibitors.

Increase in E_a (for blank 37.36 kJ and in the presence of inhibitors is 56.08-59.15kJ) with the addition of polymers indicate that physical (electrostatic) adsorption occurred in the first step which is found during adsorption processes and partially due to desorption of adsorbed inhibitor molecules from mild steel surface. The branched polymers are organic nitrogen compounds that

Table 7: Corrosion parameters for corrosion of mild steel with selected concentrations of the inhibitors in 1M H_2SO_4 by potentiodynamic polarization method

Name of the inhibitor	Concentration (ppm)	Tafel slopes (mV/dec)		E_{corr} (mV)	λ_{corr} efficiency (mAmp/cm^2)	Inhibition (%)
		b_a	b_c			
Blank	-	52	112	-467.4	1569	-
BATP	100	77	119	-530.8	792.1	49.5
	500	59	144	-490.1	445.1	71.6
	1000	63	155	-483.4	46.0	97.1
BAAZ	100	68	149	-501.7	581.7	62.9
	500	63	151	-489.5	427.7	72.7
	1000	44	133	-461.5	90.3	94.2
BETP	100	67	148	-495.1	522.9	66.7
	500	65	167	-485.6	448.9	71.4
	1000	50	135	-469.7	172.4	89.0
BEAZ	100	69	148	-509.1	621.0	60.4
	500	72	127	-514.2	693.6	55.8
	1000	76	117	-524.8	729.8	53.5

Table: 8 AC-impedance parameters for corrosion of mild steel for selected concentrations of the inhibitors in 1M H_2SO_4

Name of the inhibitor	Concentration (ppm)	R_t (ohm cm^2)	C_{dl}(μF/cm^2)	Inhibition efficiency (%)
Blank	-	11.06	27.8	-
BATP	100	34.72	28.6	68.2
	500	51.05	32.2	78.3
	1000	79.63	25.4	86.1
BAAZ	100	29.83	31.0	62.9
	500	42.93	27.5	74.2
	1000	50.82	21.3	78.2
BETP	100	22.16	31.2	37.2
	500	31.09	30.8	64.4
	1000	43.78	32.6	74.7
BEAZ	100	17.12	27.0	35.4
	500	22.97	29.5	51.9
	1000	27.41	31.7	59.7

easily get protonated to a cationic form in acid medium. The E_a value was greater than 20 kJ mol^{-1} in the presence of the inhibitor, which reveals that the entire process is controlled by the surface reaction[28].

Calculated free energies ($\Delta G°_{ads}$) are given in Table 6. The negative values of $\Delta G°_{ads}$ indicate spontaneous adsorption of polymers onto the mild steel surface[29] and strong interactions between inhibitor molecules and the metal surface[30]. Generally, values of $\Delta G°_{ads}$ up to -20 kJ mol^{-1} are consistent with the strong electrostatic interaction between charged molecules and charged metal (physisorption), while those around -40 kJ mol^{-1} or higher are associated with chemisorption as a result of the sharing or transfer of electrons from organic molecules to the metal surface to form a coordinate bond [31]. In the present study, the estimated $\Delta G°_{ads}$ values is around -28-33 kJmol^{-1} indicating that the adsorption mechanism of the polymers tested may be of mixed type involving physisorption and chemisorption, wherein physisorption predominates.

The calculated values of heat of adsorption ($\Delta H°$) and entropy of adsorption ($\Delta S°$) are listed in the Table 6. The heat of adsorption ($\Delta H°$) can be considered as the standard adsorption heat ($\Delta H°$) under the experimental conditions[32, 33]. The negative values of heat of adsorption ($\Delta H°$) indicate that the adsorption of both inhibitors is an exothermic process. It is reported that an exothermic adsorption process resembles either physisorption or chemisorption, while the endothermic adsorption process is applicable to chemisorptions[34]. The negative values of ($\Delta H°$) also suggest that inhibition efficiency (I.E.) decreased with an increase in temperature. This is due to desorption of adsorbed inhibitor molecules from the mild steel surface at higher temperatures. The value of entropy of adsorption ($\Delta S°$) is negative for polymer adsorption. Since adsorption is an exothermic process, it is always supported by the decrease in entropy, which can be clearly depicted for polymers from the calculated values. Negative values of entropies "S° imply that the activated complex in the rate determining step represents an association rather than a dissociation step, meaning that a decrease in disordering takes place on going from reactants to the activated complex.

Adsorption isotherm

The adsorption characteristics of the inhibitors were also investigated by fitting data obtained for degrees of surface coverage into different adsorption isotherms including Langmuir, Frumkin, Temkin, El awardy et al., Bockris-Swinkel, Flory-Huggins and Fruendlich adsorption isotherms. The test revealed that the adsorption characteristic of the inhibitors is best described by Langmuir adsorption isotherm. The Langmuir adsorption model relates the degree of surface coverage (θ) to the concentration of an inhibitor as follows[35],

Table 9: Amount of dissolved iron present in the corrosive solution with and without inhibitors in 1M H_2SO_4 measured using atomic absorption spectrophotometer

Name of the inhibitor	Concentration (ppm)	Amount of iron content (mg/l)	Inhibition efficiency (%)
	Blank	1304.96	-
BATP	100	564.84	56.7
	1000	69.04	94.7
BAAZ	100	688.72	47.2
	1000	203.86	84.4
BETP	100	736.88	43.5
	1000	294.60	77.4
BEAZ	100	853.64	34.6
	1000	303.82	76.7

where, Kads is the adsorption coefficient, C is the molar concentration of the inhibitor. Fig. 12 represents the Langmuir isotherm plots for all the inhibitors. A straight line was obtained for the plot of C/Q versus C with slope close to one. The regression coefficient ($R^2 > 0.9999$) suggests that the adsorption of inhibitor on the mild steel surface obeyed Langmuir isotherm. This isotherm assumes that the adsorbed molecules occupy only one site and there are no interactions with other adsorbed species[36, 37].

Electrochemical measurements
Polarization studies

The inhibitive effect of branched polyamides and polyesters were studied by using
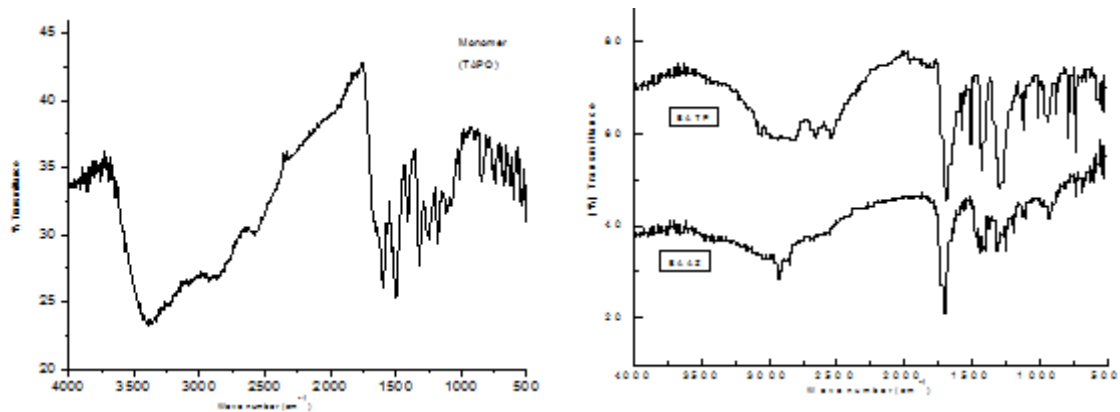
Fig. 1(a&b): FT-IR spectrum of monomer and branched polyamides
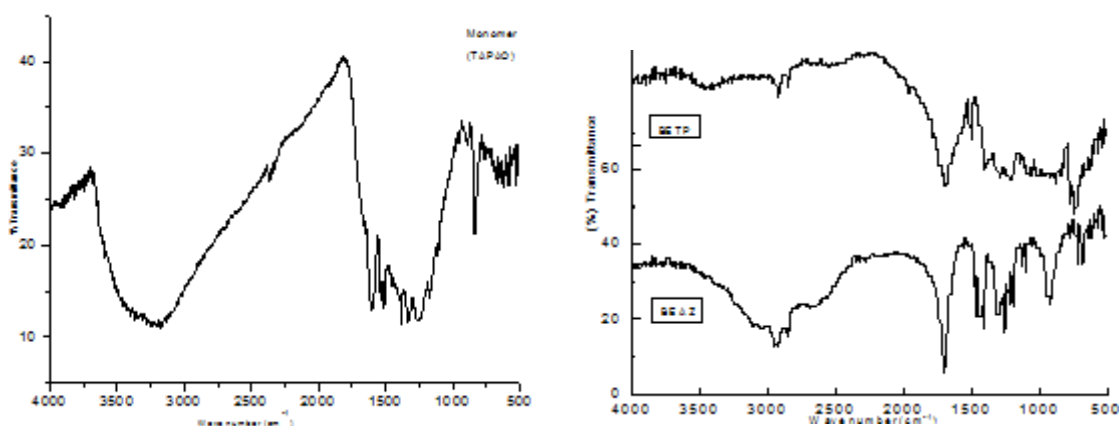
Fig. 2(a&b): FT-IR spectrum of monomer and branched polyesters
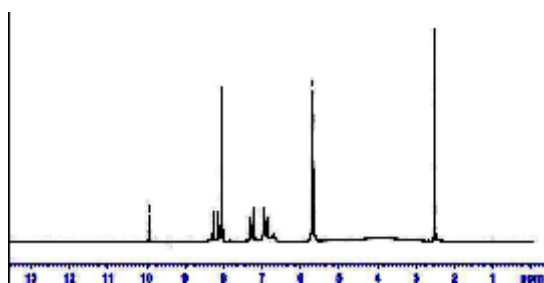
Fig. 3: ¹HNMR spectrum polyester (BETP)
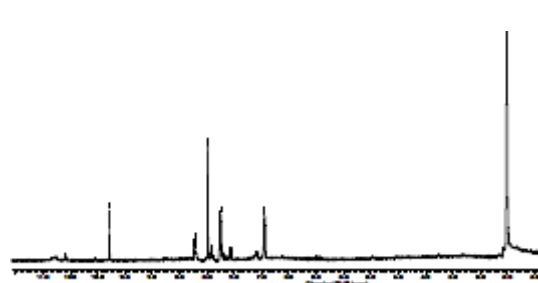
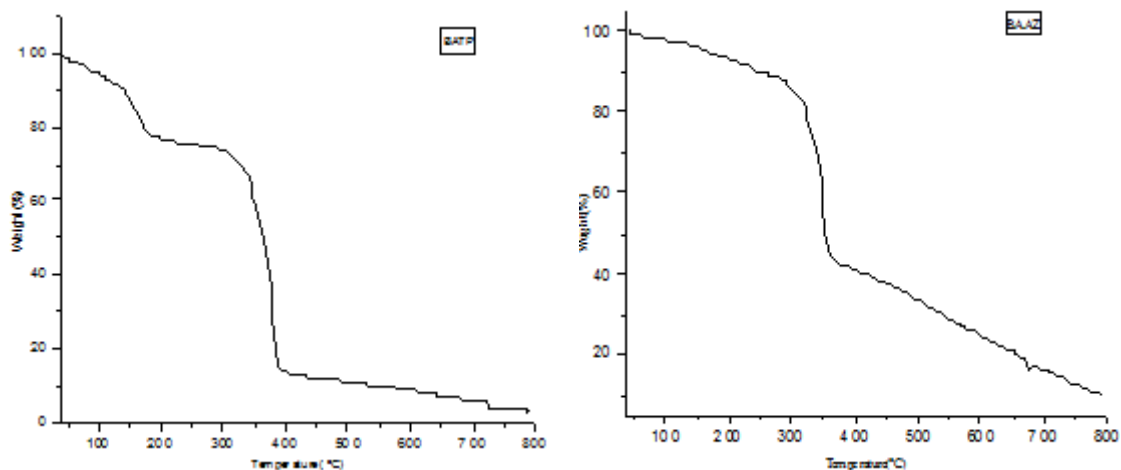**Fig. 4: ¹HNMR spectrum polyamide (BATP)**

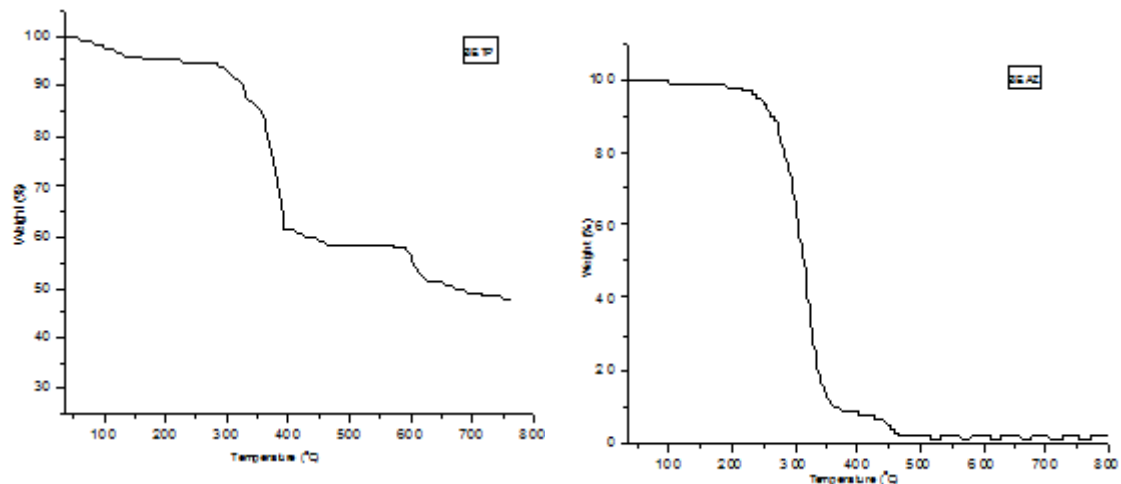**Fig. 5: Thermogravimetric curves of the polyamides**

Fig. 6: Thermogravimetric curves of the polyesters
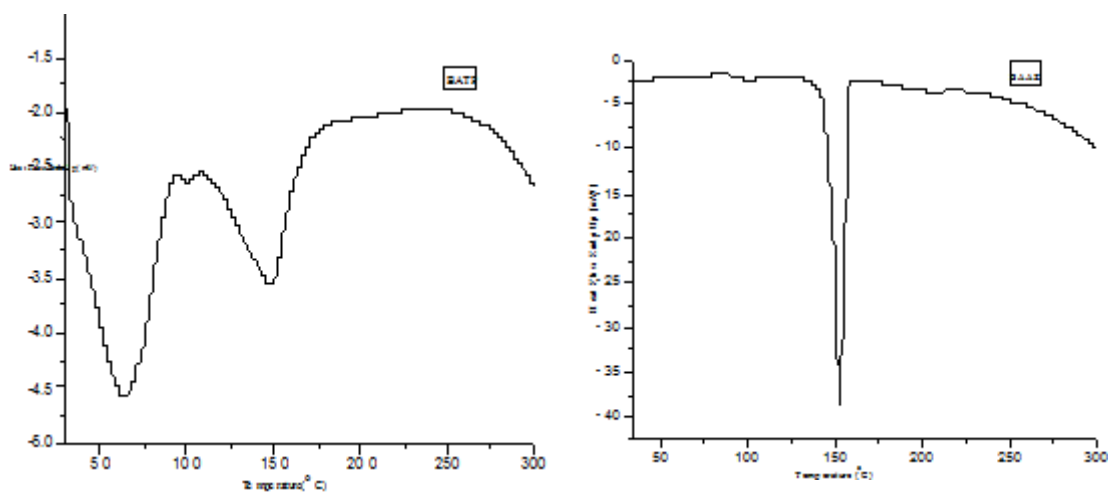

Fig. 7: DSC curves of the polyamides

potentiodynamic polarization measurements. Cathodic and anodic polarization curves of mild steel in 1M H_2SO_4 solution, in the absence and presence of various concentrations of polyamide (BATP) is shown in Fig.13. Whereas, their

corresponding electrochemical parameters such as corrosion current density (I_{corr}), anodic (b_a) and cathodic (b_c) Tafel constants, corrosion potential (E_{corr}) and inhibition efficiency (IE) are listed in Table 7. From Fig.13, it is evident that both the cathodic
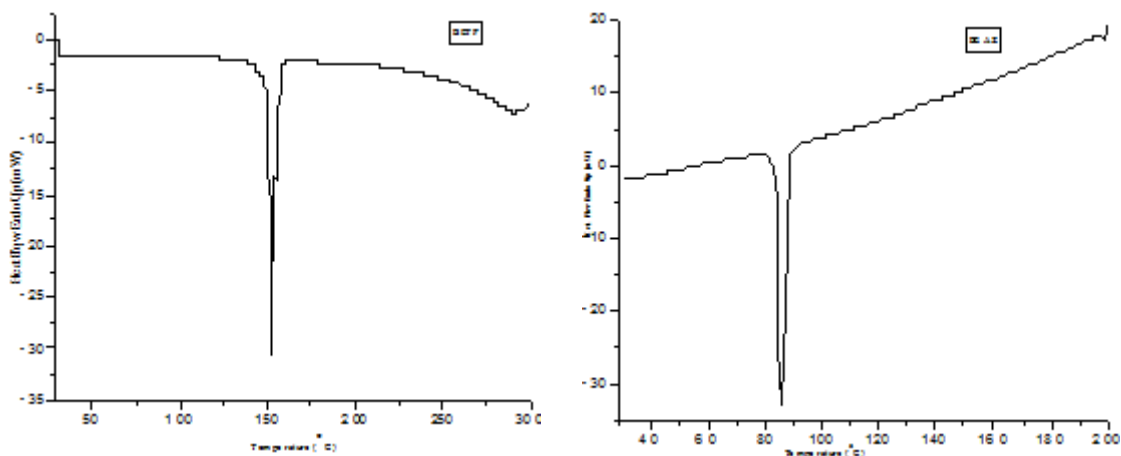

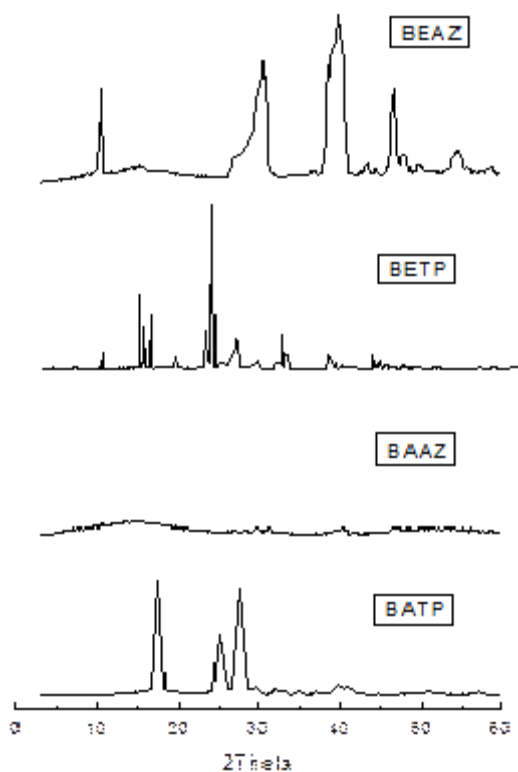**Fig. 8: DSC curves of the polyesters**

Fig. 9: Powder XRD of polymers

and anodic curves showed lower current density values in the presence of both polymers than those recorded in their absence (BATP, BAAZ, BETP and BEAZ). This confirmed the adsorption of polymers on the mild steel/acid solution interface and consequently inhibits the corrosion process [38, 39]. Moreover, Fig. 13 also suggest that the studied polymers influence both anodic as well cathodic corrosion processes; this statement is further supported from the values of anodic (b_a) and cathodic (b_c) Tafel constants and corrosion potential (E_{corr}). From Table 7, it is evident that the addition of both polymers changes the values of E_{corr} towards anodic direction both b_a and b_c are affected but b_a to a greater extent, hence polymers can be considered as mixed type but slightly anodic in nature. However, on the addition of polymers the maximum displacement in E_{corr} values was 69 mV which suggests that inhibitors act as mixed type inhibitors with predominant anodic effectiveness as it is well known that if the displacement in E_{corr} is >85 mV, the inhibitor is recognized as a cathodic or anodic type inhibitor and if the displacement of E_{corr} is <85 mV, the inhibitor is of mixed type[40, 41].

Electrochemical impedance spectroscopy

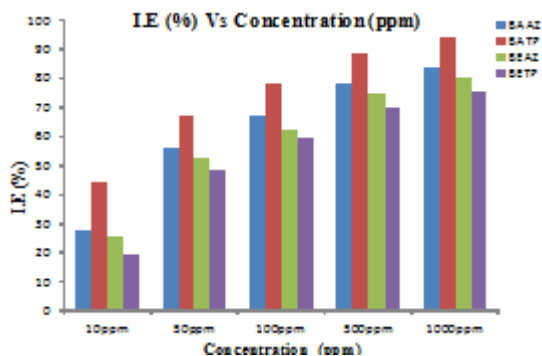Electrochemical impedance spectroscopy

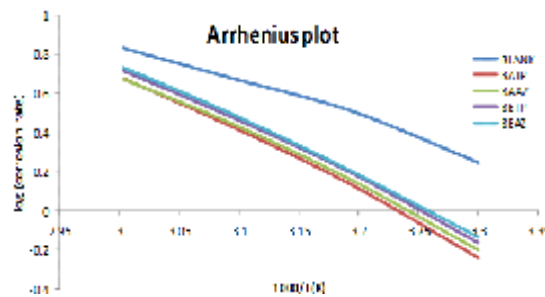**Fig.10 Plot of inhibition efficiency (%) Vs concentration (ppm) for the inhibition of corrosion of mild steel in 1M H$_2$SO$_4$**

Fig. 11: Arrhenius plot of corrosion of mild steel in 1M H$_2$SO$_4$ medium in the absence and presence of inhibitors
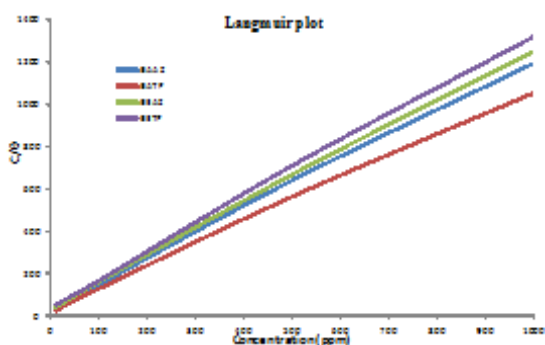

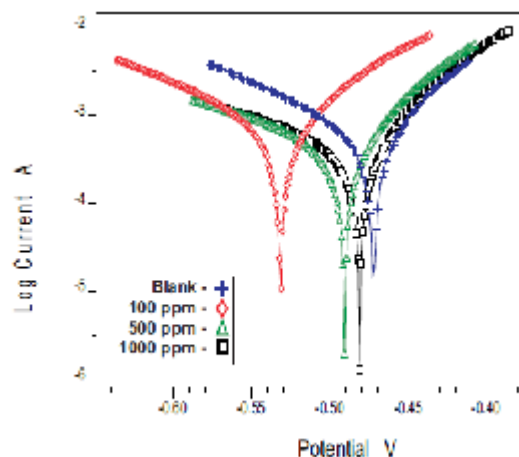**Fig. 12: Langmuir of the branched polymers**

Fig.13: Polarization curves for mild steel recorded in 1M H$_2$SO$_4$ of selected concentrations of the inhibitor (BATP)
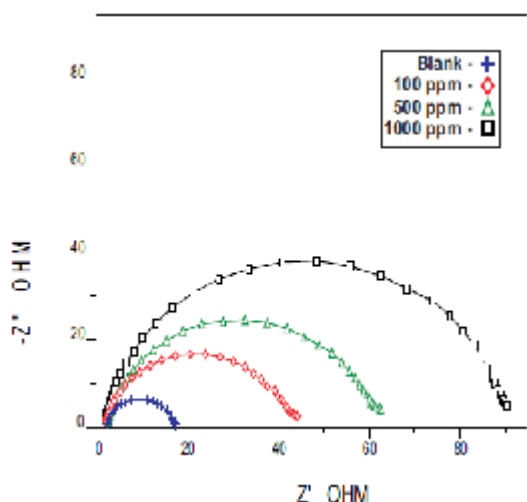

Fig.14 Nyquist diagram for mild steel in 1M H$_2$SO$_4$ for selected concentrations of inhibitor (BATP)

is a well-established and powerful tool in the study of corrosion[42]. It provides information on the metal surface properties, kinetics of the electrochemical processes at the metal/solution interface and gives evidence of inhibitor adsorption (i.e. mechanistic information) from the impedance spectra. The corrosion inhibition results of mild steel in 1M H$_2$SO$_4$ solution in the presence and absence of polymers was studied by EIS measurements at room temperature after an exposure period of 30 minutes. Figs.14 and Table 8 shows the Nyquist plot obtained from impedance data. The impedance spectra depicted depressed semicircles. These semicircles are referred to as capacitive loops. The diameter found by the intercept of each of these loops and the horizontal Z$_{real}$ axis defines the charge
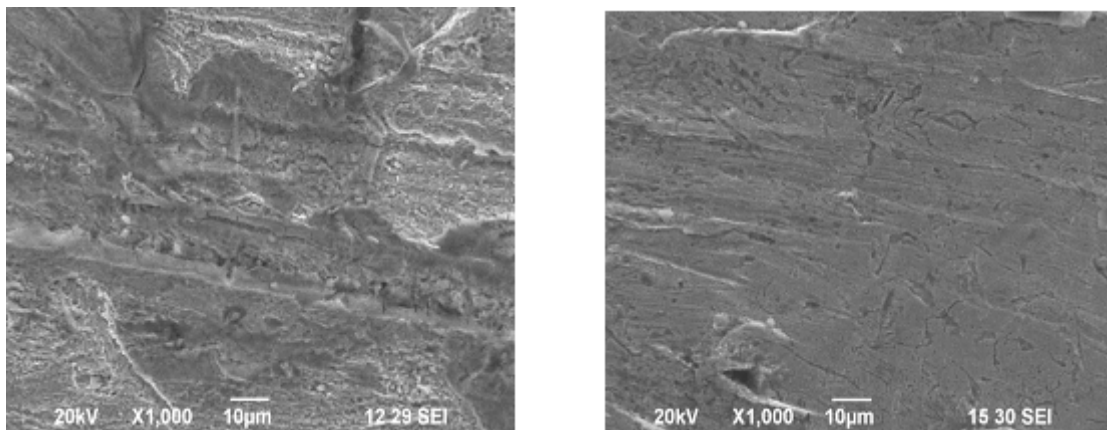
**Figs. 15(a&b): Scanning electron microscopy photographs in
the absence and presence of the inhibitor (BATP)**

transfer resistance (R_{ct}). The value of charge transfer resistance obtained is a measure of electron transfer across the metal surface and is inversely proportional to corrosion rate. Hence, a large R_{ct} value indicates a strong resistance against corrosion. In the present study R_{ct} values increased with increase in inhibitors concentration. This result indicates a decrease in the reactive surface area caused by the adsorption of the inhibitor on the mild steel surface, thus preventing the corrosion process.

Atomic Absorption Spectrophotometric Studies (AAS)

The inhibitor efficiency (%) of the polyesters (BETP & BEAZ) and polyamides (BATP & BAAZ) were calculated from the percentage of Fe dissolved obtained from AAS and the data are presented in (Table 9). The inhibitor efficiency (%) obtained by this technique was found to be in good agreement with that obtained from the conventional weight loss method.

Surface Morphology

Scanning electron microscope (SEM) has become an important tool to study surface morphology of corroded and uncorroded metals[43]. To establish the interactions of inhibitors with mild steel samples, the SEM images were recorded for mild steel in the absence and presence of optimum inhibitor concentration and results are shown in Fig. 15. Fig. 15a represents the SEM image of mild steel in the absence of polymers which is

characterized by very rough surface with pits and cracks. This suggests that mild steel surface is strongly damaged by acidic solutions in the absence of the polymers. On the other hand, Fig. 15b represents the SEM micrographs of mild steel in the presence of optimum concentration (1000 ppm) of inhibitor (BATP) in 1M H_2SO_4 for a period of 3 hrs. The image suggested that mild steel surface is fully covered with the BATP molecules and a protective BATP film is formed. This finding supports the weight loss, impedance and polarization studies.

Mechanism of inhibition

Adsorption of polymers on metal surface depends on parameters such as mode of adsorption, active sites on metal surface, planarity of molecules, free lone pairs present on heteroatoms, concentration of inhibitor etc. Normally the adsorption of inhibitor on metal surface and formation of protective layer to prevent corrosion can be understood by three ways. The first is the electrostatic interaction of protonated inhibitor molecules with already adsorbed sulphate ions (physisorption). At lower concentration, protonated molecules get adsorbed on the surface of mild steel through electrostatic interaction. With increasing concentration protonated inhibitor molecules turn to neutral molecules due to slower rate of hydrogen evolution having free lone pair electrons and promote chemical adsorption. Second way deals with the free lone pairs of heteroatoms and vacant d orbitals of Fe of mild steel (chemisorption). Third

method is the interaction of d-electrons from Fe of mild steel with the vacant orbital of inhibitor molecule (reterodonation)[44, 45]. The inhibitor molecules having d orbital electrons have both the tendency to donate and to accept free electrons and form stable chelates and behave as effective inhibitors. The presence of N-atom in the polymers form pÀ–dÀ bonds resulting in transfer of 3d-electrons from Fe atom to the vacant 2p orbital of N-atom, which enhances adsorption process on metal surface due to strong back bonding. The studied polymers have hetero atoms, aromatic rings, long chain, which get adsorbed on metal surface and form a layer to prevent direct contact of metal with aggressive media and slow down corrosion rate of metal[46].

CONCLUSION

Branched polymers have been synthesized and used as corrosion inhibitors for mild steel in 1M sulfuric acid medium. The results from FTIR, TGA, DSC and powder XRD studies confirmed the formation of branched polymers. The results of weight loss and electrochemical measurements show that branched polyamides have an excellent inhibiting property for acidic corrosion of mild steel. Inhibition efficiency increases in the order BATP, BAAZ, BETP, and BEAZ. BATP is the best inhibitor with inhibition efficiency H" 95%. This is generally attributed to the increase in the number of adsorption sites which allow higher inhibition. The synthesized branched polymers obey Langmuir adsorption isotherm. Potentiodynamic polarization measurements showed that all the polymers function as mixed-type inhibitors, retarding both anodic and cathodic reactions at the same time. The results obtained from different techniques were in good agreement with each other. The relative surface coverage of polyamide (BATP) has been verified by SEM measurements.

REFERENCES

1. E. Bayol, E.; A. A. Gurten, A. A.; Dursun, M.; K. Kayakirilmaz, K, *Acta Phys. Chim. Sin.* **2008,** *24*, 2236

2. Alsabagh, A. M.; Migahed, M. A.; Awad, H. S, *Corros. Sci.* **2006,** *48*, 813

3. Srikanth, A. P.; Lavanya, A.; Nanjundan, S.; Rajendran, N, *Appl. Surf. Sci.* **2006,** *253*, 1810

4. Hojatollah Jafari, Iman Danaee, Hadi Eskandari, Mehdi Rashvand Avei, *Ind. Eng. Chem. Res.* **2013**, *52*, 6617

5. Sitashree Banerjee, Abhinay Mishra, Madan M. Singh, Biswajit Maiti, Biswajit Ray, Pralay Maiti, *RSC Advances.* **2011,** *1*, 199

6. Arukalam, I.O.; Alaohuru, C.O.; Ugbo, C.O., Jideofor, K.N.; Ehirim, P.N.; Madufor, I.C, *Int. J. Applied Sci. Eng. Res.* **2014**, *3*, 241.

7. Manivel, P.; Venkatachari, G, *J. Appl. Polym. Sci.* **2007,** *104*, 2595

8. Amin, M. A.; Abd El-Rehim, S. S.; El-Sherbini, E. E. F.; Hazzazi, O. A, *Corros. Sci.* **2009**, *51*, 658

9. Chetouani, A.; Medjahed, K.; Sif-Lakhdar, K. E.; Hammouti, B.; Benkaddour, M.; Mansari, A, *Corros. Sci.* **2004**, *46*, 2421

10. Jeyaprabha, C.; Sathiyanarayanan, S.; Phani, K. L. N.; Venkatachari, G, *Appl. Surf. Sci.* **2005**, *252*, 966

11. Jeyaprabha, C.; Sathiyanarayanan, S.; Phani, K. L. N.; Venkatachari, G, *J.Electroanal. Chem.* **2005,** *585*, 250

12. Srivastava, S.; Banerjee, M.; Singh, M, *J. Appl. Polym. Sci.* **2010,** *116*, 810

13. Amin, M.A.; Abd El-Rehim, S.S.; El-Sherbini, E.E.F.; Hazzazi, O.A.; Abbas, M.N, *Corros. Sci.* **2009,** *51*, 658

14. Jeyaprabha, C.; Sathiyanarayanan, S.; Phani, K.L.N.; Venkatachari, G, *Appl. Surf. Sci.* **2005,** *252*, 966

15. Umoren, S.A, *Open Corros. J.* **2009,** *2*,175

16. Shukla, S.K.; Quraishi, M.A.; Prakash, R, *Corros. Sci.* **2008,** *50*, 2867

17. Yurt, A.; Buetuen, V.; Duran, B, *Mater. Chem. Phys.* **2007**, *105*, 114

18. Ion Sava, Mariana Dana Iosip, Maria Bruma, CorneliuHamciuc, Jenifer Robison, Lidia Okrasa and TadeuszPakula, *European polymer journal.* **2003**, *39*, 725

19. Mylsamy Sivadhayanithy, Lingam Ravikumar, T.Ramachandran, *Int. J. Appl. Chem.* **2007,** *3*, 245

20. Elena Hamciuc, CorneliuHamciuc, Ion sava,

Maria Bruma, *European Polymer Journal.* **2001,** *37*, 287

21. Mariana Dana Iosip, Maria Bruma, Inga Ronova, Marta Szesztay, Peter Muller, *European Polymer Journal.* **2003,** *39*, 2011.

22. Mylsamy Sivadhayanithy, Lingam Ravikumar, T. Ramachandran, *J. Chil. Chem. Soc.* **2007,** *52*, 1230

23. Oguzie, E.E.; Enenebeaku, C.K.; Akalezi, C.O.; Okoro, S.C.; Ayuk, A.A.; Ejike, E.N, *J. Colloid Interface Sci.* **2010**, *349*, 283

24. Achary, G.; Sachin, H.P.; Naik, Y.A.; Venkatesha, T.V, *Mater. Chem. Phys.* **2008,** *107*, 44

25. Banerjee, S.; Srivastava, V.; Singh, M.M, *Corros. Sci.* **2012,** *59*, 35

26. Singh, A.K.; Shukla, S.K.; Quraishi, M.A.; Ebenso, E.E, *J. Taiwan Inst. Chem. Eng.* **2012,** *43*, 463

27. Pavithra M, krishnegowda,; Venkatarangaiah T. Venkatesha,; Punith Kumar M. Krishnegowda,; Shylesha B. Shivayogiraju, *Ind. Eng. Chem,Res.* **2013,** *52*, 722

28. Herrag, L.; Hammouti, B.; Elkadiri, S.; Aouniti, A.; Jama, C.; Vezin, H.; Bentiss, F, *Corros. Sci.* **2010,** *52*, 3042

29. Tang, L.; Li, X.; Lin, L.; Mu, G.; Liu, G, *Mater. Chem. Phys.* **2006**, *97*, 301

30. ZOR. Sibel.; Pinar Dogan.; Birgul Yazici, *Corros. Rev.* **2005**, *23* , 217

31. Moretti, G.; Guidi, F.; Grion, G, *Corros. Sci.* **2004,** *46*, 387

32. Li, X. H.; Deng, S. D.; Fu, H.; Mu, G. N, *Corros. Sci.* **2008**, *50*, 2635

33. Zhao, T. P.; Mu, G. N.; *Corros. Sci.* **1999,** *4*, 1937

34. Durnie, W.; De Marco, R.; Kinsella, B.; Jefferson, A, *J. Electrochem. Soc.* **1999,** *146*, 1751

35. Ehteram A. Noor.; Aisha H. Al-Moubaraki.; *Mater. Chem. Phys.* **2008,** *110*, 145

36. Gulsen Avci, *Colloids and Surfaces A: Physicochemical and Engineering Aspects* **2008**, *317*, 730

37. Esmaeel Naderi.; Jafari, A.H.; Ehteshamzadeh, M.; Hosseini, M.G, *Mater. Chem. Phys.* **2009,** *115*, 852

38. Bahrami, M. J.; Hosseini, S. M. A.; Pilvar, P, *Corros. Sci.* **2010**, *52*, 2795

39. Ahmad, I.; Prasad, R.; Quraishi, M. A, *Corros. Sci.* **2010**, *52*, 1474

40. Satapathy, A. K.; Gunasekaran, G.; Sahoo, S. C.; Amit, K.; Rodrigues, P.V, *Corros. Sci.* **2009**, *51*, 2848

41. Kalaiselvi, P.; Chellammal, S.; Palanichamy, S.; Subramanian, G, *Mater. Chem. Phys.* **2010,** *120*, 643

42. De Sousa, F.S.; Spinelli, A, *Corros. Sci.* **2009**, *51*, 642

43. Gopiraman, M.; Sakunthala, P.; Kesavan, D.; Alexramani, V.; Kim, I.S.; Sulochana, N, *J. Coat. Technol. Res.* **2012,** *9*, 15

44. Sanatkumar, B.S.; Nayak, J.; Shetty, A. N, *Int. J. Hydrogen Energy.* **2012,** *37*, 9431

45. Ahamad, I.; Gupta, C.; Prasad, R.; Quraishi, M.A, *J Appl. Electrochem.* **2010**, *40*, 2171

46. Ahamad, I.; Prasad, R.; Quraishi, M.A, *Corros. Sci.* **2010**, *52*, 1472.